

Supporting Information:

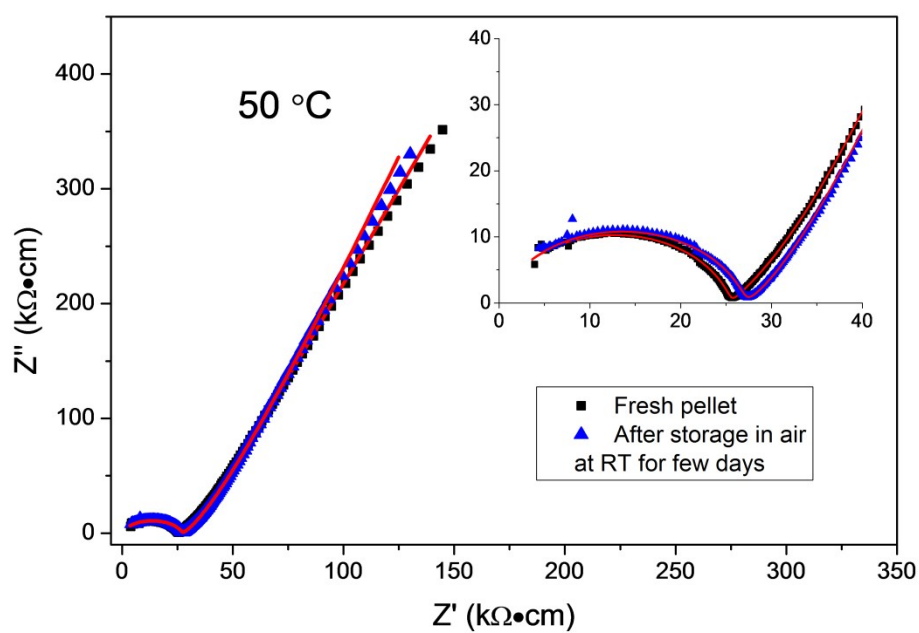


Figure S1. Impedance plots of a freshly prepared LZP-1100 pellet and the same pellet after storage in air (at room temperature) for few days, at $50\text{ }^\circ\text{C}$ (Au electrodes).

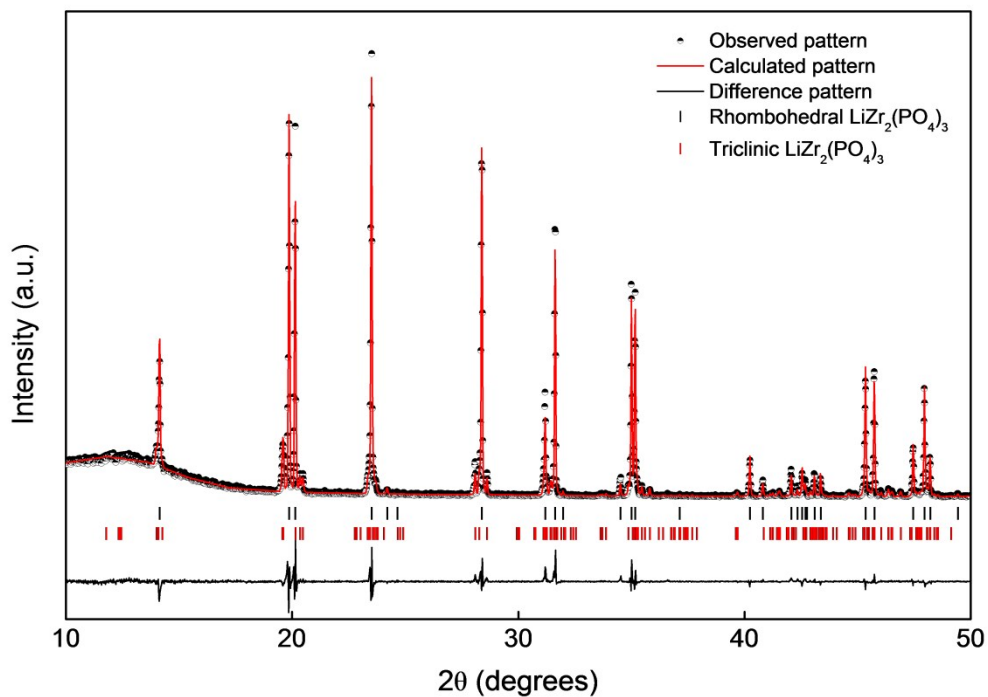


Figure S2. Rietveld fit to XRD data for L郑-1100 at room temperature; space group $R\bar{3}c$, $a = 8.8620(2)$ Å, $c = 22.1550(5)$; $\chi^2 = 3.817$; $wRp = 0.1464$, $Rp = 0.1046$. The refined weight percent of the triclinic phase is 16.2(4)%

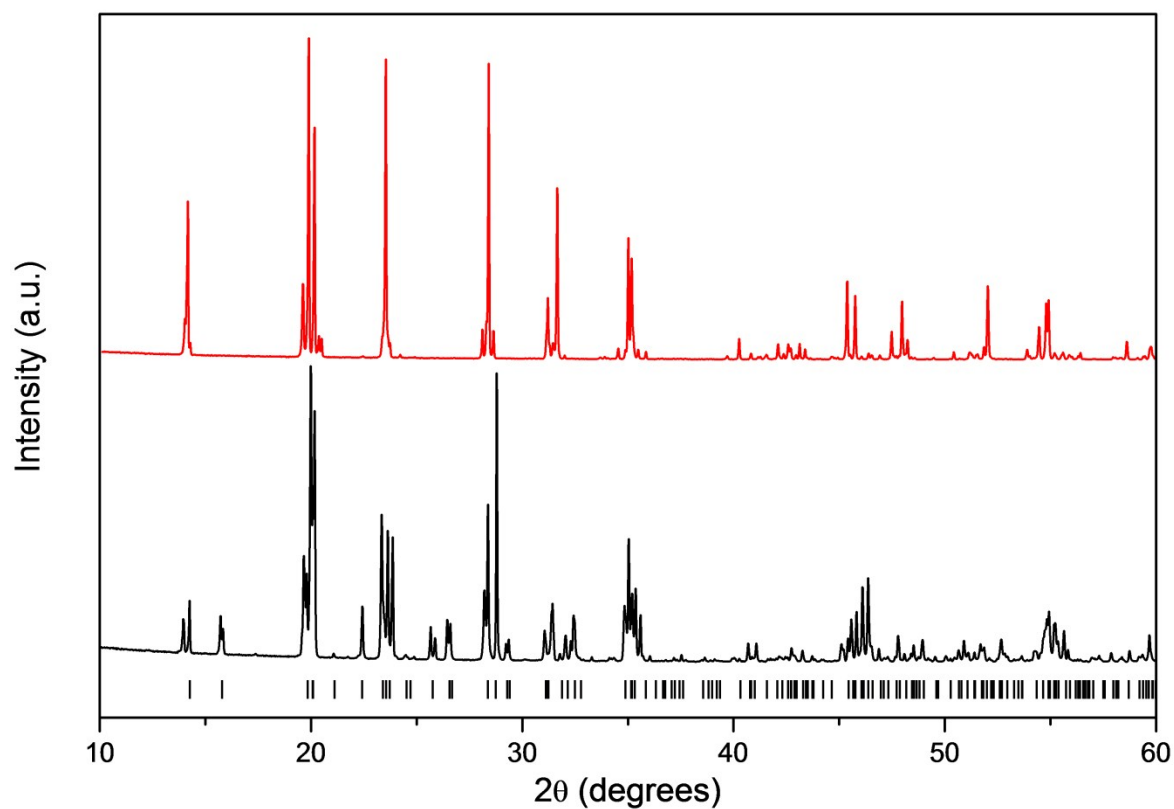


Figure S3. XRD patterns of LQP quenched from 1000 °C (bottom) and LQP quenched from 1100 °C (top). The markers are for orthorhombic LQP.

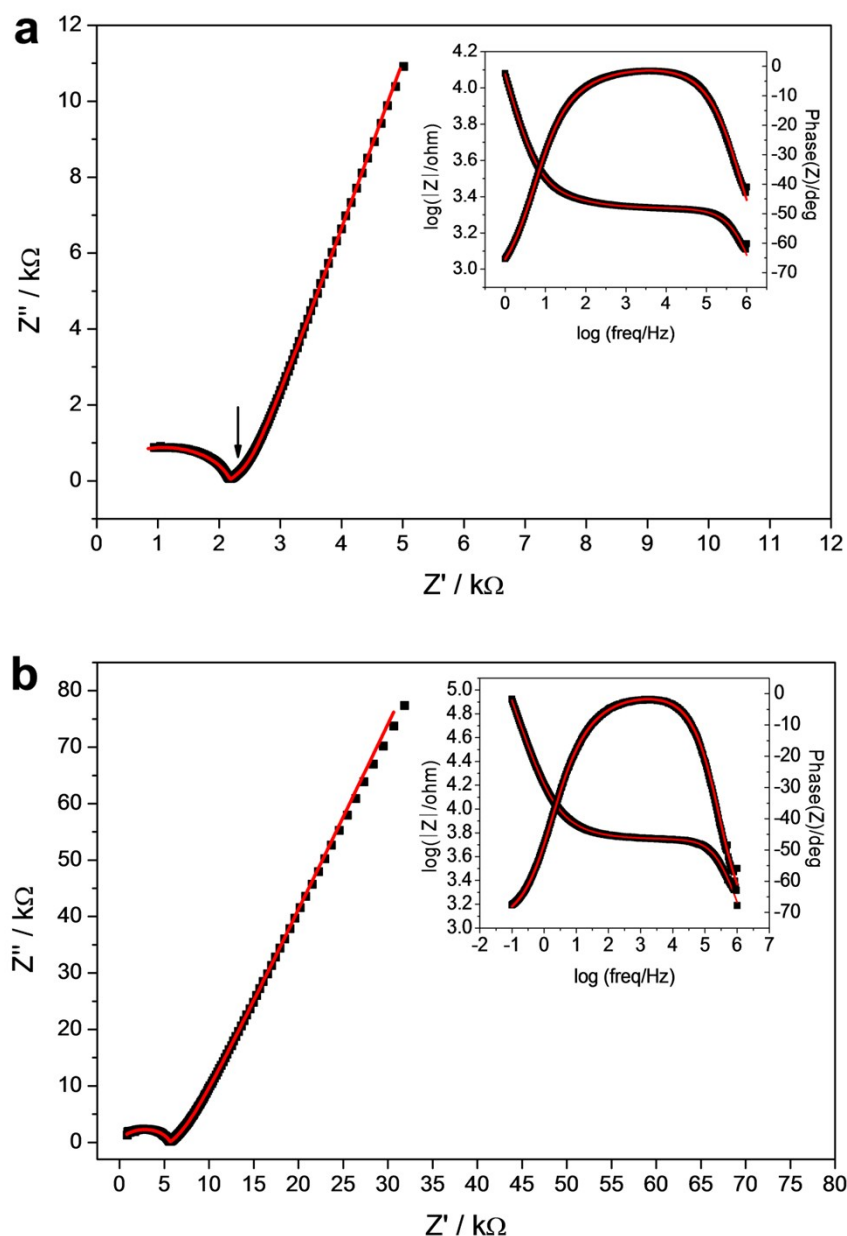


Figure S4. Nyquist and Bode impedance plots of LZP-1100, using gold electrodes, at 80 °C (a) and 50 °C (b). Data were fitted using the equivalent circuit $[R_1Q_1][R_2Q_2][Q_3]$. The use of two RQ elements $[R_1Q_1]$ and $[R_2Q_2]$ was necessary to obtain reasonable fits and correspond to fitting the observed high-frequency semicircle and a very small subsequent mid-frequency semicircle (indicated by the arrow in the figure), respectively. The refined capacitances for the $[R_1Q_1][R_2Q_2]$ elements are: 8.0×10^{-10} F ($\alpha=0.865$) and 1.9×10^{-5} F ($\alpha=0.858$) for data collected at 80 °C, and 7.3×10^{-10} F ($\alpha=0.863$) and 1.8×10^{-5} F ($\alpha=0.813$) for data collected at 50 °C. The high-frequency impedance clearly corresponds to the total (bulk and grain-boundary) resistance of the pellet, while the observed high capacitances of the $[R_2Q_2]$ element suggest that the impedance observed at mid-frequencies corresponds to a surface effect. XPS analysis, however, gives no evidence of the modification of the surface by exposure to air (e.g. by formation of surface Li_2CO_3), which suggests that the surface effect observed in the impedance spectra is likely intrinsic and associated with the pellet preparation procedure. The contribution of this surface resistance to the total resistance of the pellet was $\sim 14\%$ in the case of the data collected at 80 °C.

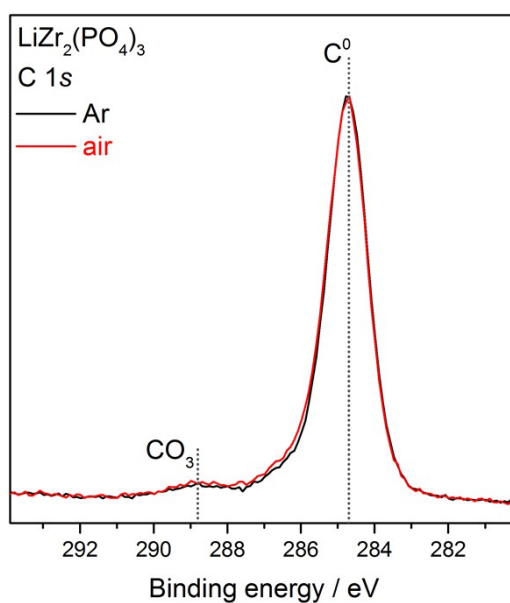


Figure S5. C 1s XPS data collected from two LZP-1100 pellets, one polished and stored in air for several days (red), and the other polished and stored under Ar in a glovebox (black). Unlike garnet-type solid electrolytes (ref 14), the data show no evidence for the accumulation of Li₂CO₃ on the surface by exposure to air, which indicates excellent stability in air.

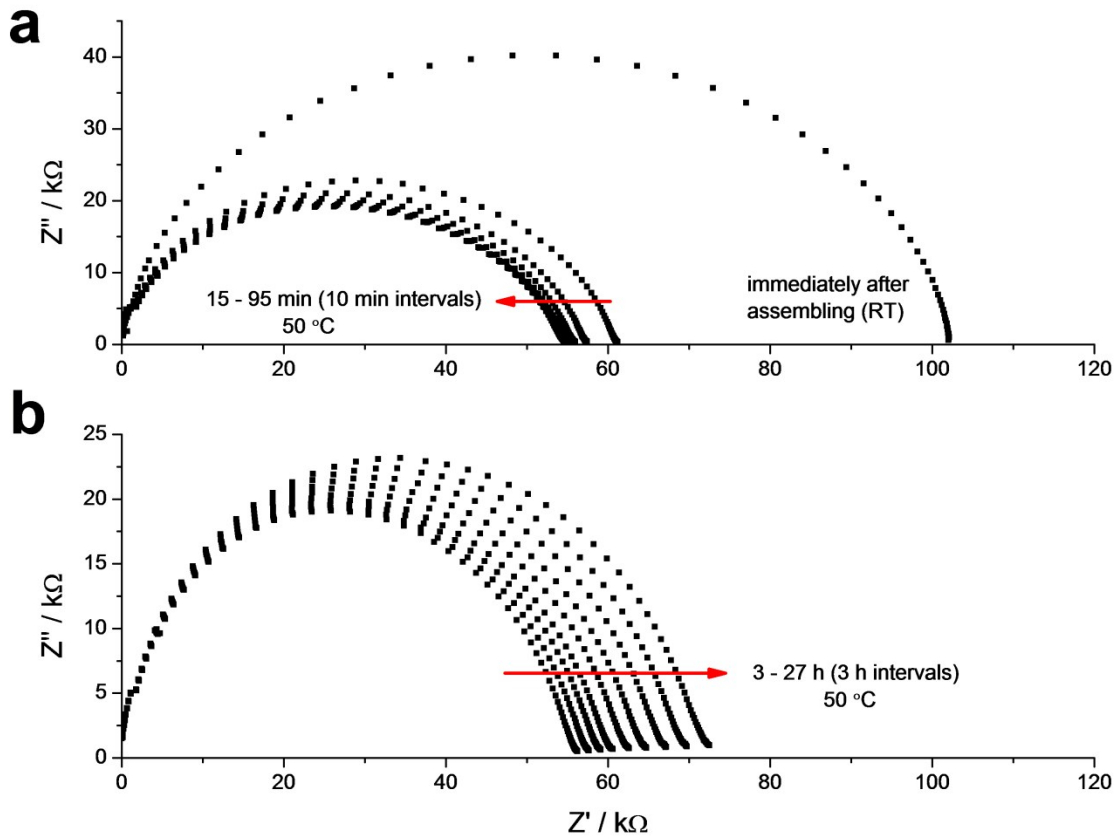


Figure S6. Time-dependent impedance spectra collected from a LZP-1100 sample using Li electrodes at 50 °C. Thermal stabilization of the symmetric cell was achieved after ~ 90 min (a), then spectra were collected from the cell at equal time intervals up to 27 h (b).

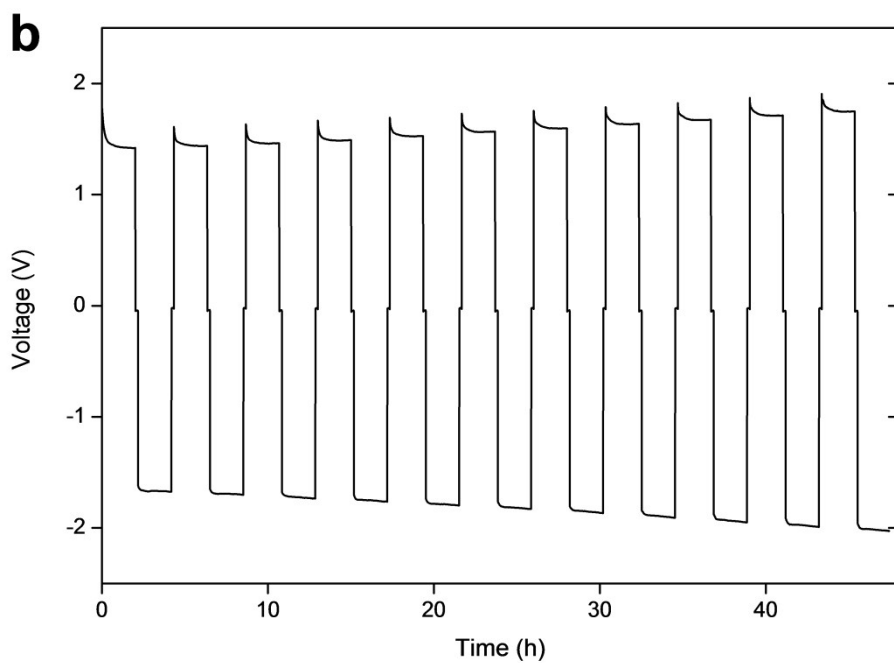
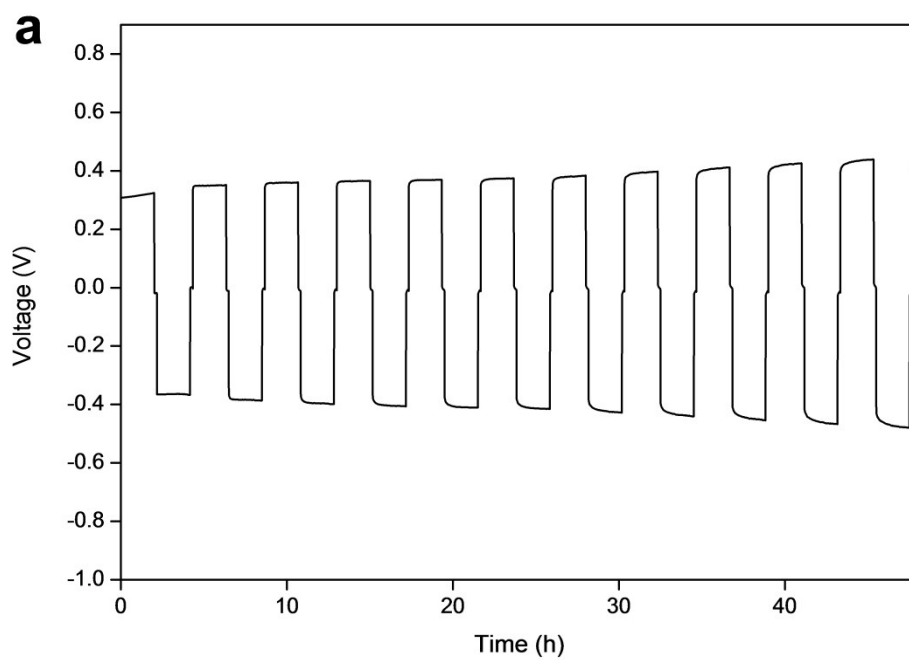


Figure S7. a) Galvanostatic cycling of the Li/LZP/Li symmetric cell using Au buffer, at 50 °C and 40 $\mu\text{A}/\text{cm}^2$ current density. b) Galvanostatic cycling of the Li/LZP/Li symmetric cell at 80 °C and 100 $\mu\text{A}/\text{cm}^2$ current density.



Figure S8. LZO pellets after galvanostatic cycling of the Li/LZO/Li symmetric cells, at 80 °C for 100 h.

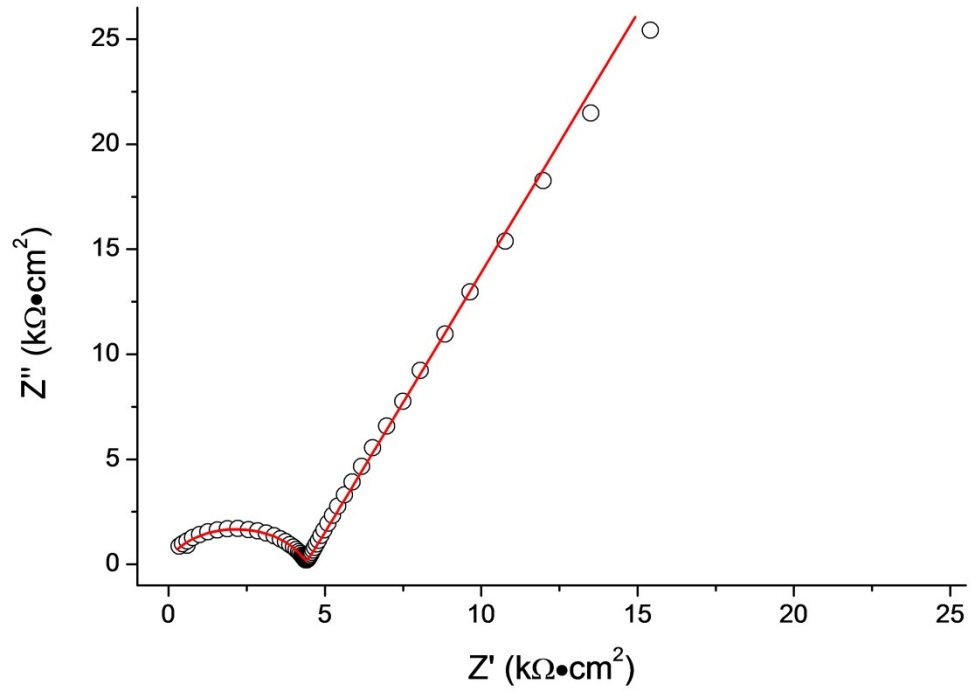


Figure S9. Impedance spectrum collected from the Li/LZP/Au cell (LZP pellet thickness ~ 1.1 mm) at 50 °C. Data were fitted using the equivalent circuit $[R_1Q_1][R_2Q_2][Q_3]$.

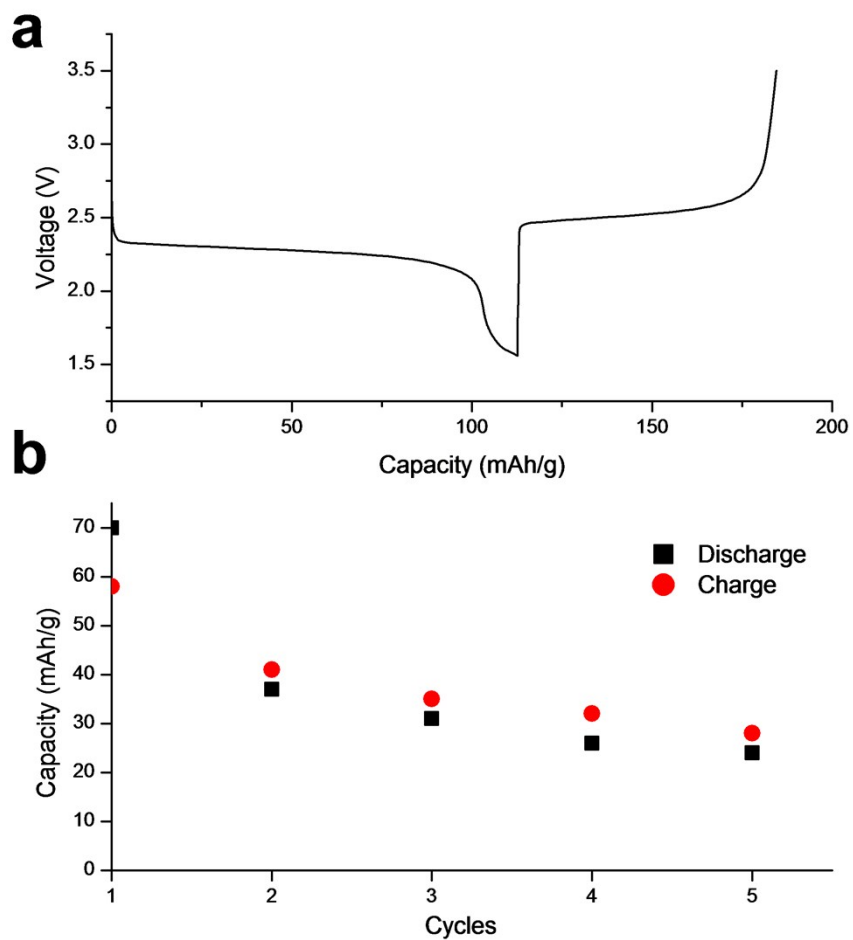


Figure S10. a) Discharge/charge profile of the Li/LZP/LTP cell at 80 °C and 20 $\mu\text{A}/\text{Cm}^2$. b) The first five cycles of the Li/LZP/LTP cell at 50 °C and 6 $\mu\text{A}/\text{Cm}^2$.

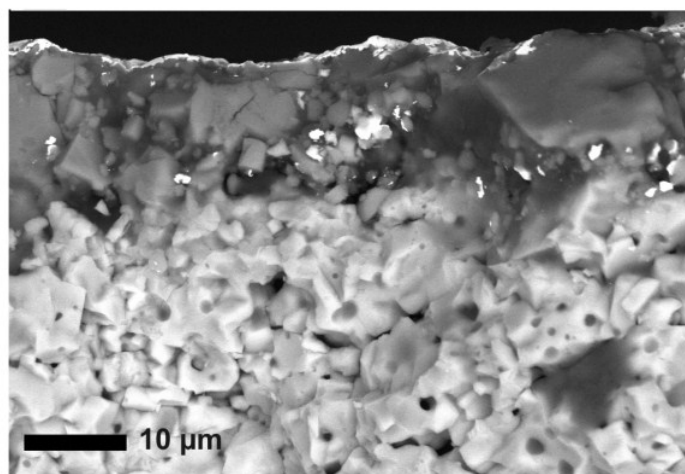


Figure S11. SEM image of a longitudinal section of the Li/LZP/LTP cell, collected using AsB detector, showing the LZP/LTP interface after cycling the cell (50 °C and 6 $\mu\text{A}/\text{Cm}^2$).